

# Each Monomer of the Dimeric Accessory Protein for Human Mitochondrial DNA Polymerase Has a Distinct Role in Conferring Processivity\*

Received for publication, September 6, 2009, and in revised form, October 18, 2009. Published, JBC Papers in Press, October 26, 2009, DOI 10.1074/jbc.M109.062752

Young-Sam Lee<sup>‡</sup>, Sujin Lee<sup>‡</sup>, Borries Demeler<sup>§</sup>, Ian J. Molineux<sup>†¶</sup>, Kenneth A. Johnson<sup>¶||</sup>, and Y. Whitney Yin<sup>¶||1</sup>

From the <sup>‡</sup>Institute for Cellular and Molecular Biology, <sup>¶</sup>Section of Molecular Genetics and Microbiology, and <sup>||</sup>Department of Chemistry and Biochemistry, University of Texas, Austin, Texas 78712 and the <sup>§</sup>Department of Biochemistry, University of Texas at San Antonio Health Sciences Center, San Antonio, Texas 78229

The accessory protein polymerase (pol)  $\gamma$ B of the human mitochondrial DNA polymerase stimulates the synthetic activity of the catalytic subunit. pol  $\gamma$ B functions by both accelerating the polymerization rate and enhancing polymerase-DNA interaction, thereby distinguishing itself from the accessory subunits of other DNA polymerases. The molecular basis for the unique functions of human pol  $\gamma$ B lies in its dimeric structure, where the pol  $\gamma$ B monomer proximal to pol  $\gamma$ A in the holoenzyme strengthens the interaction with DNA, and the distal pol  $\gamma$ B monomer accelerates the reaction rate. We further show that human pol  $\gamma$ B exhibits a catalytic subunit- and substrate DNA-dependent dimerization. By duplicating the monomeric pol  $\gamma$ B of lower eukaryotes, the dimeric mammalian proteins confer additional processivity to the holoenzyme polymerase.

Most DNA polymerases dissociate from their template DNA too rapidly for efficient replication; as a consequence, only a short DNA product is synthesized per binding event. To perform processive DNA synthesis, the catalytic subunit of a DNA polymerase associates with an accessory subunit, forming a holoenzyme that displays a markedly increased affinity for DNA. Consequently, the number of nucleotides incorporated at each binding event is significantly increased.

DNA replicases use a variety of accessory subunits for processivity enhancement. Whereas their catalytic subunits of all DNA replicases present a recognizable polymerase (pol)<sup>2</sup> core structure, the accessory subunits differ considerably in shape and size. The processivity factor  $\beta$ -sliding clamp for bacterial DNA polymerases II and III, gp45 for T4 DNA polymerase, UL44 for cytomegalovirus DNA polymerase, UL30 for herpes simplex virus I DNA polymerase, and proliferating cell nuclear antigen for eukaryotic DNA polymerases  $\delta$  and  $\epsilon$ , are all toroidal oligomeric complexes that encircle the duplex DNA (1–4). The rate of dissociation of the holoenzyme from DNA is

thereby dramatically decreased. The processivity factor for bacteriophage T7 gene 5 product protein is the small monomeric *Escherichia coli* protein thioredoxin, which increases polymerase processivity by direct DNA contact and by enhancing interactions of the catalytic subunit with the template DNA (5, 6).

The processivity factor for mitochondrial DNA polymerase, pol  $\gamma$ B, bears no resemblance to these processivity factors. It is structurally homologous to Class II aminoacyl tRNA synthetases (7) and has a unique mode of action for processivity enhancement. In the holoenzyme, pol  $\gamma$ B simultaneously increases the polymerization rate and suppresses the exonuclease activity of the catalytic subunit (8, 9). By increasing polymerization rate, more nucleotides are incorporated into the product DNA per unit time (thus per binding event).

A crystal structure of human mitochondrial DNA polymerase has shed some light on how processivity is achieved by the holoenzyme (10). pol  $\gamma$  is a heterotrimer where one molecule of pol  $\gamma$ A binds to a dimeric pol  $\gamma$ B (Fig. 1A). pol  $\gamma$ B positions the positively charged AID subdomain of pol  $\gamma$ A to bind DNA and preferentially directs the primer terminus into the polymerase active site. The structure reveals that pol  $\gamma$ A interacts primarily with one monomer of pol  $\gamma$ B and makes only limited contacts with the distal monomer. Interestingly, whereas the mammalian pol  $\gamma$ Bs are dimeric, that in *Drosophila melanogaster* is a monomer (11). The structure of human holoenzyme suggests that a monomeric pol  $\gamma$ B could be completely functional; the question then arises as to the necessity and function of a dimeric pol  $\gamma$ B in mammals.

Mutations affecting pol  $\gamma$ A are common causes of human mitochondrial diseases. The human pol  $\gamma$  structure has rationalized several disease-implicated pol  $\gamma$ A mutations that interact with the proximal pol  $\gamma$ B monomer (10). However, interpreting some specific clinical observations with the help of the holoenzyme structure suggests that both pol  $\gamma$ B monomers may be important to humans. A patient who died at 6 months of age was found to carry the R232G substitution in pol  $\gamma$ A, and other patients were found to carry R232H in *trans* with other mutations (12, 13). Arg<sup>232</sup> provides the most significant interaction between pol  $\gamma$ A and the distal pol  $\gamma$ B monomer by forming a salt bridge with Glu<sup>394</sup> of pol  $\gamma$ B (Fig. 1A) (10). Although the association of disease with mutations that disrupt the interactions between pol  $\gamma$ A and the proximal pol  $\gamma$ B monomer is easy to comprehend, any cause and effect relationship between mutations that alter the limited pol  $\gamma$ A-distal pol  $\gamma$ B monomer

\* This work was supported, in whole or in part, by National Institutes of Health Grants GM032095 (to I. J. M.), GM044613 (to K. A. J.), and GM083703 (to Y. W. Y.). This work was also supported by Welch Foundation Grants F-1604 and F-1592 (to K. A. J. and Y. W. Y., respectively). Continuing development of the UltraScan software is supported by NIH Grant RR022200 (to B. D.).

<sup>1</sup> To whom correspondence should be addressed: Institute for Cellular and Molecular Biology, University of Texas, 2500 Speedway, MBB 3.422, Austin, Texas 78712. Tel.: 512-471-5583; E-mail: whitney.yin@mail.utexas.edu.

<sup>2</sup> The abbreviations used are: pol, polymerase; nt, nucleotide(s); aaRS, aminoacyl-tRNA synthetase.

interaction is more tenuous without additional biochemical testing.

We report here that disruption of the dimeric structure of pol  $\gamma$ B decreases the stability of the human holoenzyme and abolishes the acceleration of polymerization rate. Consequently, a monomeric pol  $\gamma$ B confers less processivity to the holoenzyme. Our studies further reveal that each pol  $\gamma$ B monomer has a distinct role in promoting processive DNA synthesis.

## EXPERIMENTAL PROCEDURES

**Cloning, Expression, and Protein Purification**—All mutants and wild-type pol  $\gamma$ B were cloned into pET22b(+), and the C-terminal His-tagged constructs were expressed in *E. coli* Rosetta (DE3) (Novagen) at 37 °C in LB. Proteins were induced with 0.4 mM isopropyl 1-thio- $\beta$ -D-galactopyranoside when the cell density reached 0.6  $A_{600}$ , and the culture was subsequently incubated at a reduced temperature of 25 °C for 6 h before harvesting. The deletion mutant  $\Delta$ I4 was constructed as previously described (14). Other mutant pol  $\gamma$ Bs were constructed using the following oligonucleotides (mutation sites in bold) as primers for QuikChange (Stratagene) site-directed mutagenesis: D129K, 5'-GCAGGTATTCCC**GGT**GAAAGCCCTCCACC-ACAAACC and 5'-GGTTTGTGGTGGAGGGCT**TTT**CACCGGAATACCTGC; R107E, 5'-CCTTGGGCGTAGAGTTG**GAA**AGAACCTGGCCGCAG and 5'-CTGCGGCCAGGTTCTTT**TCCA**ACTCTACGCCCAAGG.

The C-terminal His-tagged, exonuclease-deficient catalytic subunit pol  $\gamma$ A was constructed by substituting Glu<sup>200</sup> with Ala and by deleting the mitochondrial localization sequence (residues 1–29). The *exo*<sup>-</sup> pol  $\gamma$ A gene was transferred into the baculovirus genome using the shuttle vector pBacPAK9 (Clontech) and expressed in infected Sf9 insect cells. Proteins were purified by sequential application to nickel-nitrilotriacetic acid, SOURCE S, and Superdex 200 columns (15).

**Analytical Ultracentrifugation**—All experiments were performed using a Beckman Optima XL-I. Data were analyzed with the program UltraScan v9.9,<sup>3</sup> making appropriate hydrodynamic corrections for the buffers used.<sup>4</sup> The partial specific volumes of pol  $\gamma$ B proteins, estimated from the protein sequence (18), were 0.734, 0.735, 0.736, and 0.736 cm<sup>3</sup>/g for  $\Delta$ I4,  $\Delta$ I4-D129K, D129K, and wt pol  $\gamma$ B, respectively. All samples were analyzed in 50 mM NaCl and 25 mM sodium phosphate buffer (pH 7.4).

Sedimentation velocity experiments were conducted at 40,000 rpm, 20 °C, for pol  $\gamma$ B wild-type, D129K,  $\Delta$ I4, and  $\Delta$ I4-D129K at equal loading concentrations (1.7  $\mu$ M). Scans were taken at 230 nm in intensity mode. All data, with time invariant noise subtracted, were initially analyzed by the two-dimensional spectrum method (19), and further refined with the genetic algorithm (20). Statistics were subjected to Monte Carlo analysis (21). Sedimentation coefficient distributions were cal-

culated by the method of van Holde-Weischet as previously described (22).

Sedimentation equilibrium experiments were conducted at 4 °C for pol  $\gamma$ B wild-type, mutant D129K,  $\Delta$ I4, and  $\Delta$ I4-D129K. Two sets of loading concentrations were prepared for each protein: 3.5, 5.8, and 8.1  $\mu$ M for scanning at 280 nm and 0.8, 1.3, and 1.8  $\mu$ M for 230 nm. Samples were centrifuged to equilibrium at 15,000, 18,700, 22,500, 26,200, or 30,000 rpm and scanned simultaneously at 230 and 280 nm. The resulting 30 scans were globally fitted to multiple models as described (23).<sup>5</sup> The extinction coefficient at 280 nm was determined to be 71,940 absorption unit mol<sup>-1</sup>cm<sup>-1</sup> by amino acid composition (25). The extinction coefficient at 230 nm was estimated to be 323,340 absorption unit mol<sup>-1</sup>cm<sup>-1</sup> by globally fitting wavelength scans from each concentration to sums of Gaussian terms (26). The most appropriate model was chosen based on minimum residual and the best statistics.

**Steady-state Polymerization Assay**—Polymerization assays used single-stranded M13mp18 DNA annealed to a 26-nucleotide primer (5'-GGATTATTTACATTGGCAGATTCACC). Reactions contained 80 nM pol  $\gamma$ A, 200 nM pol  $\gamma$ B (or variant), and 50 nM primer/template DNA in 20  $\mu$ l of 10 mM HEPES, pH 7.5, 80 mM KCl, 12.5 mM NaCl, 50  $\mu$ g/ml bovine serum albumin, and 3 mM  $\beta$ -mercaptoethanol. The holoenzyme titration experiment used pol  $\gamma$ A/pol  $\gamma$ B ratios of 40 nM/100 nM, 80 nM/200 nM, and 160 nM/400 nM; after preincubation at 37 °C for 5 min, 500 nM poly(dA-dT)·poly(dA-dT) was added as "trap" DNA. Reactions were then initiated by the addition of MgCl<sub>2</sub> (10 mM), dNTPs (50  $\mu$ M dGTP, dATP, and dTTP, 5  $\mu$ M dCTP, and 0.1  $\mu$ M [ $\alpha$ -<sup>32</sup>P]dCTP) and incubated at 37 °C for 10 min. Reactions were stopped by the addition of 1% SDS, 20 mM EDTA, and 0.1 mg/ml Protease K and then incubated at 42 °C for 30 min. After applying reaction mixtures to Micro Bio-Spin 6 columns (Bio-Rad) to remove free nucleotides, DNAs were heat-denatured at 95 °C for 5 min in gel loading buffer (70% formamide, 1 $\times$  Tris, boric acid, and EDTA, 100 mM EDTA), and were analyzed on a 6% polyacrylamide/7 M urea gel. Reaction products were visualized by autoradiography.

**Pre-steady-state Kinetics**—A 25/45-mer primer-template was prepared by annealing equimolar amounts of 5'-<sup>32</sup>P-labeled primer (5'-TCCTCGCAGCCGTCCAACCAACTCA) and template (5'-GGACGGCATTGGATTCGAGGTTGAGT-TGGTTGGACGGCTGCGAGGA) by heating at 95 °C for 5 min and then slowly cooling to 20 °C in 10 mM Tris-HCl (pH 8.0 at 25 °C) and 50 mM NaCl. Single-nucleotide incorporation DNA polymerization assays were performed using a RQF-3 Rapid Chemical Quench Flow instrument (KinTek Co.), where one syringe contained pol  $\gamma$ -DNA complex (140 nM pol  $\gamma$ A, 600 nM pol  $\gamma$ B (or variant), 400 nM 25/45-mer DNA, 20 mM HEPES (pH 7.5 at 25 °C), 100 mM NaCl), and the other syringe contained a nucleotide-magnesium mix (100  $\mu$ M dATP, 20 mM MgCl<sub>2</sub>, 20 mM HEPES (pH 7.5 at 25 °C), 100 mM NaCl). The reaction was initiated by rapidly mixing equal volumes from

<sup>3</sup> B. Demeler (2009) An Integrated Data Analysis Software Package for Sedimentation Experiments. University of Texas Health Science Center at San Antonio, Dept. of Biochemistry.

<sup>4</sup> T. M. Laue, B. D. Shah, T. M. Ridgeway, and S. L. Pelletier (1992) Computer-aided Interpretation of Analytical Sedimentation Data for Proteins. Analytical Ultracentrifugation in Biochemistry and Polymer Science, Royal Society of Chemistry, Cambridge, United Kingdom.

<sup>5</sup> B. Demeler (2005) UltraScan: A Comprehensive Data Analysis Software Package for Analytical Ultracentrifugation Experiments. Modern Analytical Ultracentrifugation: Techniques and Methods, Royal Society of Chemistry, United Kingdom.

## Processivity Enhancement by Dimerization of Accessory Subunit

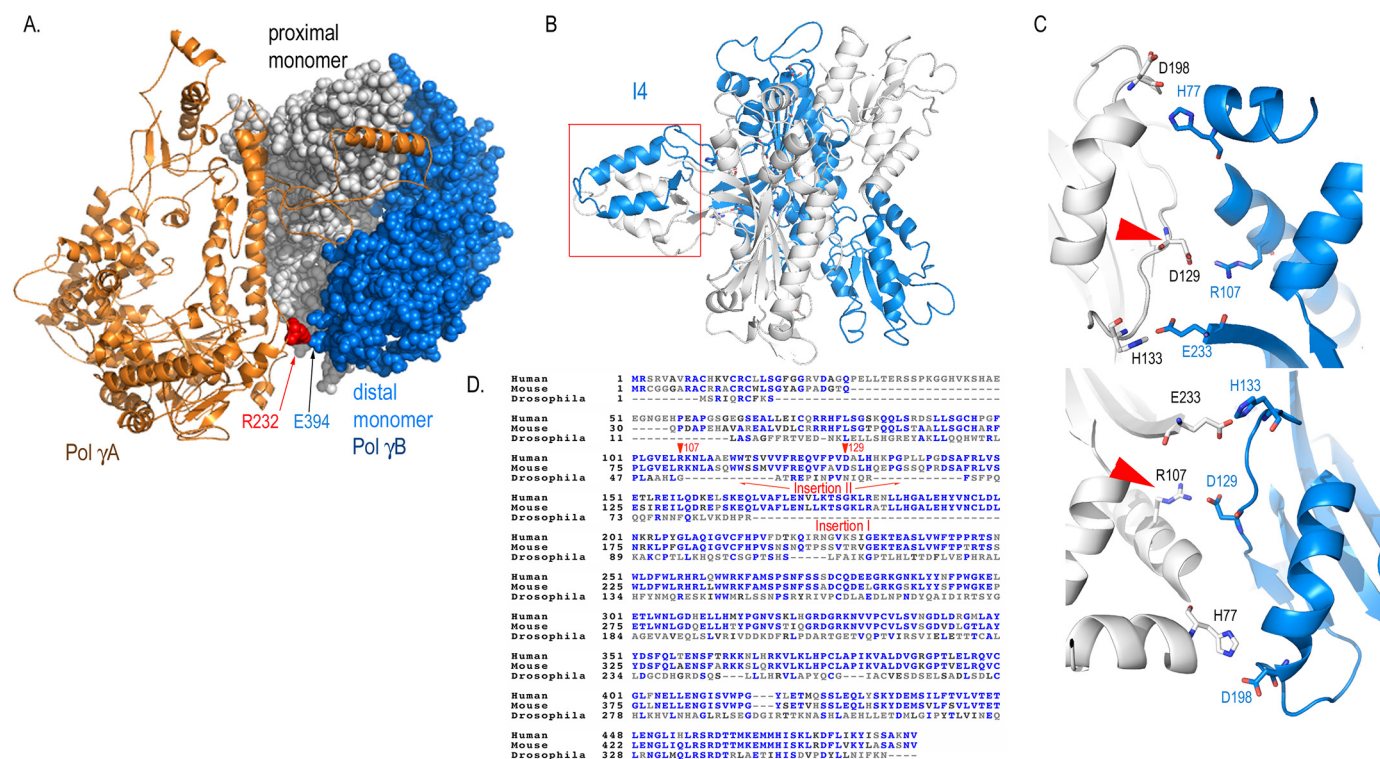


**FIGURE 1. Structural and bioinformatic basis for construction of pol  $\gamma$ B variants.** A, structure of a trimeric human pol  $\gamma$  holoenzyme shows pol  $\gamma$ A forms extensive interactions with the proximal pol  $\gamma$ B monomer but limited contacts with the distal monomer. Alignment of human, mouse, and *Drosophila* pol  $\gamma$ B reveals two inserted regions (D). One forms a four-helical bundle I4 (B); the second forms interdimer H-bonds (C). Both regions are important for dimerization of mammalian pol  $\gamma$ B.

each syringe at 37 °C for 5, 10, 20, 30, 40, 60, 80, 100, 250, and 500 ms, and 1, 2.5, and 5 s and quenched with 0.5 M EDTA. Quenched reaction samples were applied to a 15% polyacrylamide/7 M urea gel. The 26-mer DNA product was visualized by autoradiography and quantified with software Quantity One (Bio-Rad). The time dependence of the product formation was fit to the burst equation (Equation 1).

$$[\text{product}_{26\text{-mer}}] = A(1 - e^{-k_{\text{pol}} \cdot t}) + k_{\text{ss}} \cdot t \quad (\text{Eq. 1})$$

**Analytical Gel Filtration**—Each pol  $\gamma$ B variant (2  $\mu$ M monomer) was analyzed alone, with 1  $\mu$ M pol  $\gamma$ A, or with 1  $\mu$ M pol  $\gamma$ A and 3  $\mu$ M 25/30-mer (5'-GCATCTACGACCACTCATACACCT/3'-AAAGGAGGTGTATGAGTTGGTCGTA-GATGC) primer/template DNA on a Superdex 200 10/300 GL column. Samples (300  $\mu$ l) were applied to the column in 20 mM HEPES (pH 7.5 at 25 °C), 140 mM KCl, 1 mM EDTA (pH 8.0), 5 mM  $\beta$ -mercaptoethanol and eluted at a flow rate of 0.65 ml/min. Eluates were monitored at  $A_{280}$  and  $A_{260}$ , and proteins were visualized by Coomassie staining after SDS-PAGE.

## RESULTS

**Construction and Preparation of pol  $\gamma$ B Variants**—In contrast to the monomeric *Drosophila* pol  $\gamma$ B, the human protein is a homodimer. To investigate the function of each human pol  $\gamma$ B monomer, we constructed a monomeric pol  $\gamma$ B, expecting to detect differences in activity between pol  $\gamma$ A alone and its complex with a monomeric pol  $\gamma$ B (heterodimer AB holoenzyme), or with the dimeric pol  $\gamma$ B (heterotrimer AB<sub>2</sub> holoenzyme).

Guided by bioinformatic, structural, and prior biochemical analyses, we identified two regions that contribute to pol  $\gamma$ B dimerization. In comparison to the monomeric *Drosophila* pol  $\gamma$ B, the human protein has two insertions that are located in the dimer interface (Fig. 1, B and D): Insertion I contains residues 165–201, which is part of the four-helical bundle (147–180) formed with the same region from another monomer. The region has been termed I4, and a mutant lacking it has been termed  $\Delta$ I4 (Fig. 1B) (14). Insertion II contains residues Arg<sup>107</sup>–Val<sup>119</sup> and His<sup>133</sup>–Ala<sup>146</sup>. This region in human pol  $\gamma$ B harbors cross-dimer hydrogen bonds formed by Asp<sup>129</sup>–Arg<sup>107</sup>, His<sup>77</sup>–Asp<sup>198</sup>, and His<sup>133</sup>–Glu<sup>233</sup>, each of which is duplicated by the 2-fold symmetry axis relating the two pol  $\gamma$ B monomers (Fig. 1C). The Asp<sup>129</sup>–Arg<sup>107</sup> salt bridges should be particularly strong, because they include both H-bonding and charge-charge interactions.

Hypothesizing that both regions are necessary for dimerization, we constructed four human pol  $\gamma$ B mutants where the regions are disrupted either individually or jointly:  $\Delta$ I4 removes the four-helical bundle by replacing residues 147–179 with a Gly-Gly dipeptide. D129K converts the Asp<sup>129</sup>–Arg<sup>107</sup> electrostatic attraction to repulsion by substituting Asp with Lys at position 129.  $\Delta$ I4-D129K combines the I4 deletion and the D129K substitution. Lastly, anticipating altered activity from mutant  $\Delta$ I4-D129K, we constructed  $\Delta$ I4-D129K/R107E, where two substitutions, D129K and R107E, were added to the  $\Delta$ I4 construct. These substitutions replace the wild-type Asp<sup>129</sup>–Arg<sup>107</sup> pair with a new salt bridge Lys<sup>129</sup>–Glu<sup>107</sup>. All proteins were purified to high homogeneity (Fig. 2A).

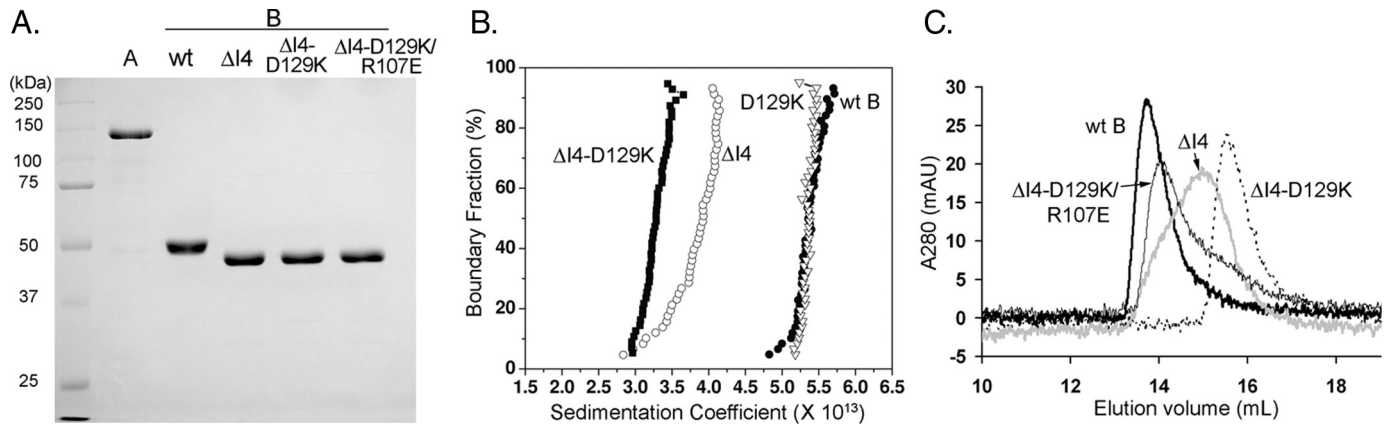


FIGURE 2. **Variant pol  $\gamma$ B oligomeric states.** A, purified pol  $\gamma$ B proteins (1  $\mu$ g) analyzed on a SDS-PAGE gel and stained with Coomassie Blue R-250. B, superimposed van Holde-Weischet integral distribution plots of wild-type (filled circles), D129K (open triangles),  $\Delta$ I4 (open circles), and  $\Delta$ I4-D129K (filled squares). C, superimposed chromatograms of pol  $\gamma$ B variants (2  $\mu$ M) analyzed on a Superdex 200 10/300 GL column: wt pol  $\gamma$ B (thick black line),  $\Delta$ I4 (gray line),  $\Delta$ I4-D129K (dotted line), and  $\Delta$ I4-D129K/R107E (thin black line).

**Oligomerization of pol  $\gamma$ B Variants**—Dimerization of pol  $\gamma$ B mutant proteins was first evaluated by analytical ultracentrifugation. We performed sedimentation velocity experiments under identical conditions using pol  $\gamma$ B wild-type, D129K,  $\Delta$ I4, and  $\Delta$ I4-D129K proteins. Both pol  $\gamma$ B wild-type and mutant D129K have the same weight-average sedimentation coefficient of 5.37, indicating that they have identical oligomeric states (Fig. 2B).  $\Delta$ I4 has a weight-average sedimentation coefficient of 3.74 and shows a typical monomer-dimer equilibrium pattern that is consistent with a weak dimer. Mutant  $\Delta$ I4-D129K gave a weight-average sedimentation coefficient 3.28, consistent with it being completely monomeric under these conditions.

To obtain quantitative measurements of dimer formation and dissociation, we analyzed the proteins by sedimentation equilibrium centrifugation. Mutant  $\Delta$ I4 best fit a reversible monomer-dimer equilibrium model with a dissociation constant of 16.6  $\mu$ M, in agreement with the previously reported value of 7  $\mu$ M (15). All other pol  $\gamma$ B variants were best fit by a single species model, because only a very low level of other species was detected. Wild-type pol  $\gamma$ B was calculated to have a molecular mass of 114.1 kDa, and mutant D129K of 99.5 kDa; both values are consistent with the proteins being dimers of a 52.5-kDa protein (by sequence). The mutation D129K therefore appears to have little effect on dimer formation. Conversely, the molecular mass of  $\Delta$ I4-D129K was estimated to be 50 kDa, consistent with it being monomeric. To estimate the  $K_d$  boundary values for these variants, the missing species (monomer for the wild-type and mutant D129K, and dimer for  $\Delta$ I4-D129K) were assumed to be below the detection limit ( $A_{230} < 0.05$  absorption units). Data for all pol  $\gamma$ B variants are summarized in Table 1.

The oligomeric states of pol  $\gamma$ B and variants were independently confirmed by gel-filtration chromatography, extrapolating from their elution volumes and their calculated molecular weights. All proteins were analyzed at 2  $\mu$ M, a minimum concentration that is dictated by the system's UV detection limit (20 absorption units at 280 nm). Wild-type pol  $\gamma$ B elutes with an apparent molecular mass of 100 kDa (Fig. 2C), consistent with it being a dimer.  $\Delta$ I4 elutes as a broadened peak, suggestive

TABLE 1

Dissociation constants measured by analytical ultracentrifugation

pol $\gamma$ B proteins	$K_d^a$	Molecular mass <sup>b</sup>	Oligomeric state
	$\mu$ M	kDa	
Wild-type	<0.1	92.9 (89.5, 94.7)	Dimer
D129K	<0.1	91.1 (90.8, 92.0)	Dimer
$\Delta$ I4	16.6	90.9 (90.7, 91.3) 78.1 (77.8, 79.1)	Monomer/dimer mixture
$\Delta$ I4-D129K	>200	43.8 (43.6, 44.1)	Monomer
$\Delta$ I4-D129K/R107E	ND <sup>c</sup>		Monomer/dimer mixture

<sup>a</sup> Measured by analytical ultracentrifugation using the sedimentation equilibrium method.

<sup>b</sup> Based on genetic algorithm-Monte Carlo analysis of sedimentation velocity data.

Values in parenthesis are 95% confidence intervals.

<sup>c</sup> ND, not determined.

of it being a mixture of 50- and 100-kDa species that correspond to monomers and dimers, and  $\Delta$ I4-D129K behaves as a 50-kDa monomer. However, when  $\Delta$ I4-D129K bears the additional R107E substitution, it chromatographs as a dimer. Thus, the D129K-R107E combination, which restores the salt-bridge interaction between two pol  $\gamma$ B monomers, also restores the ability to form a dimer that may be even stronger than  $\Delta$ I4. This result therefore clearly demonstrates the importance of the salt bridge between residues 129 and 107 in pol  $\gamma$ B dimer formation.

These analyses suggest that alteration of either dimer-stabilization region alone is insufficient to dissociate dimeric pol  $\gamma$ B completely under the conditions of our analyses, but together they abolish all significant intermolecular interactions. The  $K_d$  for dimerization of pol  $\gamma$ B  $\Delta$ I4-D129K is more than 2000 times higher than that of the wild-type, and the mutant protein can therefore be considered monomeric under our conditions of analysis. Because the construction of pol  $\gamma$ B  $\Delta$ I4-D129K was predicated on the structure of the dimeric human protein and sequence alignment differences with *Drosophila* pol  $\gamma$ B, these data also explain why the latter protein is a monomer.

**Effects of pol  $\gamma$ B Dimerization on Processive DNA Synthesis**—On primed M13 DNA, most products synthesized by pol  $\gamma$ A are <100 nt, but, as expected for a processivity factor, when pol  $\gamma$ A forms a holoenzyme with wild-type pol  $\gamma$ B, they increase in length severalfold and become more abundant (Fig. 3A). Similar results are seen when pol  $\gamma$ A complexes with pol  $\gamma$ B  $\Delta$ I4,

## Processivity Enhancement by Dimerization of Accessory Subunit

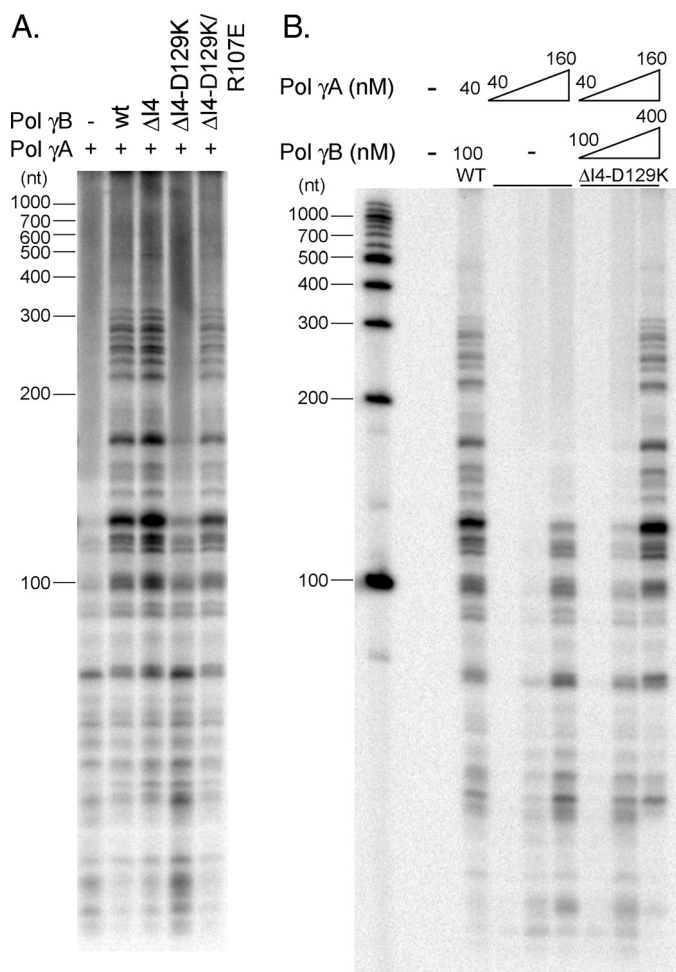


**FIGURE 3. Steady-state DNA polymerization assays.** pol  $\gamma$ A with or without pol  $\gamma$ B (wild-type or a variant) were analyzed using M13mp18 DNA annealed to a 26-nt primer. *A*, reaction products were visualized on a polyacrylamide denaturing gel. Reactions contained 80 nM pol  $\gamma$ A, 200 nM pol  $\gamma$ B or a variant, 50 nM primer-template DNA, and 10-fold excess of trap DNA. *B*, reactions were performed with pol  $\gamma$ A either alone at 40, 80, and 160 nM, or in the presence of  $\Delta$ I4-D129K at concentrations of pol  $\gamma$ A/ $\Delta$ I4-D129K 40 nM/100 nM, 80 nM/200 nM, or 160 nM/400 nM. pol  $\gamma$ A/wild-type pol  $\gamma$ B 40 nM/100 nM served as the control.

suggesting that the latter is fully competent to stimulate DNA synthesis in this system. Removal of the four-helical bundle, thereby weakening formation of the pol  $\gamma$ B dimer, has little effect. These results are comparable to previous studies comparing wild-type and  $\Delta$ I4 pol  $\gamma$ B (15).

In contrast, the monomeric pol  $\gamma$ B  $\Delta$ I4-D129K is much less effective; although a small increase in total products was observed relative to pol  $\gamma$ A alone, there was little increase in product length (Fig. 3A). These data suggest that loss of the distal pol  $\gamma$ B monomer diminishes holoenzyme processivity. In agreement with this conclusion, when using pol  $\gamma$ B  $\Delta$ I4-D129K/R107E, where the salt bridge and dimerization capability is restored, the resulting holoenzyme exhibits activity comparable to the wild-type or  $\Delta$ I4-containing enzyme.

To test whether the deficiency of the monomeric pol  $\gamma$ B is due to an intrinsic lack of activity or to a weakened interaction between subunits, holoenzyme containing monomer pol  $\gamma$ B was titrated in a polymerization assay. Activities comparable to the wild-type holoenzyme were observed at concentration

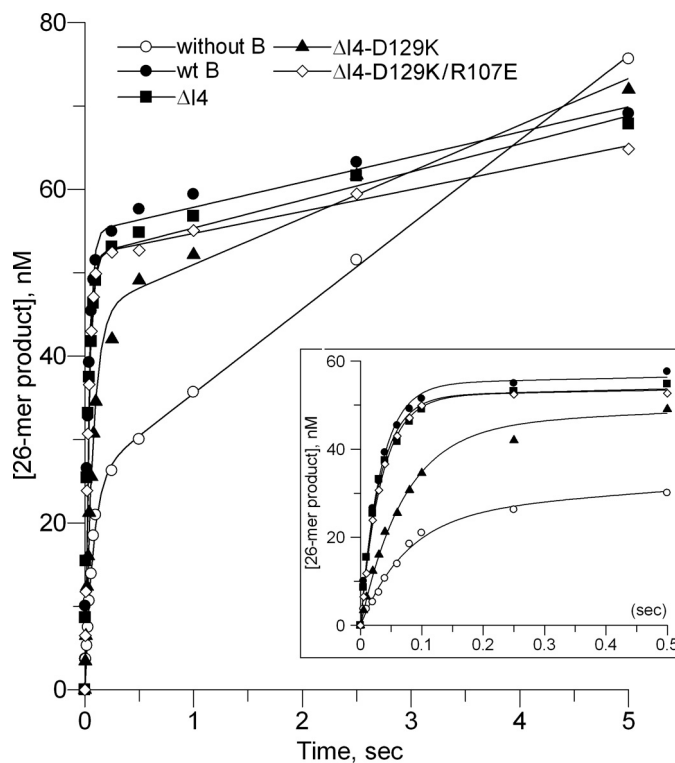


**FIGURE 4. Time-dependent product formation in pre-steady-state assays.** The 26-mer products were quantified from reactions of pol  $\gamma$ A without or with pol  $\gamma$ B variants and plotted against time; without pol  $\gamma$ B (open circles), wt pol  $\gamma$ B (filled circles),  $\Delta$ I4 (filled squares),  $\Delta$ I4-D129K (filled triangles), and  $\Delta$ I4-D129K/R107E (open diamonds). Shorter time points are shown as an inset. Reactions contained 70 nM pol  $\gamma$ A,  $\pm$ 300 nM pol  $\gamma$ B wild-type or a variant, 200 nM 25/45-mer DNA, 10 mM  $MgCl_2$ , and 50  $\mu$ M dATP.

4-fold higher concentration (160 nM, Fig. 3B).  $\Delta$ I4-D129K at this concentration remains a monomer, and we show below that the corresponding holoenzyme is an AB heterodimer. This indicates that loss of function in  $\Delta$ I4-D129K is likely caused either by impaired subunit interactions or by impaired interactions of holoenzyme with DNA.

**Pre-steady-state Kinetics Analysis of pol  $\gamma$ B Variants**—To gain a better mechanistic insight of pol  $\gamma$ B oligomerization on the polymerization reaction, we used pre-steady-state kinetics to examine single nucleotide incorporation to a 25-mer primer annealed to a 45-mer template (25/45-mer). Identical experiments were carried out with 70 nM pol  $\gamma$ A, either with or without 300 nM pol  $\gamma$ B wild-type,  $\Delta$ I4,  $\Delta$ I4-D129K, or  $\Delta$ I4-D129K/R107E proteins, 200 nM DNA substrate 25/45-mer. A pre-equilibrated pol·DNA complex was rapidly mixed with 50  $\mu$ M dATP and 10 mM  $MgCl_2$ . The time dependence for formation of the 26-mer product was plotted against time (Fig. 4), and data were then fitted to the burst equation:  $[\text{product}_{26\text{-mer}}] = A(1 - e^{-k_{\text{pol}}t}) + k_{\text{ss}} \cdot t$ , where  $A$ , the burst amplitude, reflects the amount of productive protein·DNA complex that can be turned over in the first cycle of the reaction, and  $k_{\text{pol}}$ , the burst rate, denotes the fast polymerization rate in the first cycle of the reaction. We should note that  $k_{\text{pol}}$  is not the initial slope, or the first order derivative of the curve, because  $(d[\text{product}])/dt = A \cdot k_{\text{pol}}$  when  $t \rightarrow 0$ , before steady-state conditions apply. The initial slope is thus the product of the two parameters  $A$  and  $k_{\text{pol}}$ . Finally,  $k_{\text{ss}}$ , the steady-state turnover rate, is the slope of the

**TABLE 2**  
Pre-steady state kinetic parameters for pol  $\gamma$ B variants

	pol $\gamma$ A				
	Wild-type pol $\gamma$ B	pol $\gamma$ B $\Delta$ I4	pol $\gamma$ B $\Delta$ I4-D129K	pol $\gamma$ B $\Delta$ I4-D129K/R107E	
Amplitude $A$ (nM)	25.40 $\pm$ 0.70	54.83 $\pm$ 0.70	52.00 $\pm$ 0.80	45.40 $\pm$ 1.06	52.09 $\pm$ 0.39
Burst rate $k_{\text{pol}}$ ( $\text{s}^{-1}$ )	13.38 $\pm$ 0.91	30.99 $\pm$ 1.24	31.56 $\pm$ 1.52	14.07 $\pm$ 0.81	29.32 $\pm$ 0.68
Steady state rate $k_{\text{ss}}$ ( $\text{nM}\cdot\text{s}^{-1}$ )	10.13 $\pm$ 0.26	3.01 $\pm$ 0.30	3.36 $\pm$ 0.34	5.58 $\pm$ 0.40	2.62 $\pm$ 0.16
$k_{\text{off}}^a$ ( $\text{s}^{-1}$ )	0.40	0.05	0.06	0.12	0.05
Processivity <sup>b</sup> (nt)	33	620	526	117	586

<sup>a</sup> Calculated as  $k_{\text{off}} = k_{\text{ss}}/A$ .<sup>b</sup> Processivity was calculated as  $k_{\text{pol}}/k_{\text{off}}$ . The standard deviations are residual errors from least-square model fitting.

linear steady-state phase of the reaction. Other parameters are computed from the primary experimental data: the off-rate,  $k_{\text{off}} = k_{\text{ss}}/A$ , reflects the frequency at which polymerase dissociates from its template, and the equation, processivity =  $k_{\text{pol}}/k_{\text{off}}$  gives the number of nucleotides incorporated before dissociation. The kinetic parameters for pol  $\gamma$ B, both wild-type and variants, are summarized in Table 2.

In the presence of wild-type pol  $\gamma$ B, the burst amplitude of pol  $\gamma$ A increases from 25 to 55 nM, showing that pol  $\gamma$ B increases the formation of a productive protein-DNA complex 2-fold; the burst rate increases from 13 to 31  $\text{s}^{-1}$ , indicating that pol  $\gamma$ B also accelerates the polymerization rate (Table 2). In addition,  $k_{\text{ss}}$  is reduced 3-fold, indicating a lower steady-state turnover rate. The lower the value of  $k_{\text{ss}}$ , the less likely is polymerase to dissociate from its template. This means that the polymerase can catalyze more rounds of nucleotide incorporation, thereby becoming more processive, before it dissociates from the template. The combination of an increased polymerization rate and a reduced  $k_{\text{off}}$  due to the presence of a wild-type dimeric pol  $\gamma$ B in holoenzyme, results in an increase in processivity from 33 nt by pol  $\gamma$ A alone to 650 nt, a 20-fold enhancement. Pre-steady-state data (Table 2) using pol  $\gamma$ B- $\Delta$ I4 and pol  $\gamma$ B- $\Delta$ I4-D129K/R107E show that these proteins have similar properties to wild-type.

The monomeric pol  $\gamma$ B  $\Delta$ I4-D129K confers different kinetic properties from a dimeric pol  $\gamma$ B. Although pol  $\gamma$ B  $\Delta$ I4-D129K increases the amplitude of the reaction to nearly the same level as the wild-type protein (from 25 to 45 nM), it is unable to accelerate the burst rate (Table 2). Accordingly, the monomeric pol  $\gamma$ B increases processivity only from 33 to 117 nt, a mere  $\sim$ 3.5-fold. To test whether the slightly reduced amplitude of  $\Delta$ I4-D129K, which is  $\sim$ 90% of wild-type, was caused by a reduced interaction with pol  $\gamma$ A, we repeated the experiment at double the  $\Delta$ I4-D129K concentration. The amplitudes are the same for  $\Delta$ I4-D129K at 300 or 600 nM, (45.4 and 45.5 nM, respectively), suggesting the reduction is not due to a reduced interaction with pol  $\gamma$ A, rather that a monomeric pol  $\gamma$ B is slightly inferior to a dimer in stimulating formation of a productive pol-DNA complex. Importantly, no change of burst rate was observed (14.1  $\text{s}^{-1}$  and 16.3  $\text{s}^{-1}$  at 300 nM and 600 nM, respectively) compared with pol  $\gamma$ A alone (13.4  $\text{s}^{-1}$ ), showing that monomeric pol  $\gamma$ B has little or no ability to accelerate the rate of synthesis by pol  $\gamma$ A.

**Effect of pol  $\gamma$ A on pol  $\gamma$ B Dimerization**—All the activity assays for holoenzyme containing pol  $\gamma$ B- $\Delta$ I4 were conducted at concentrations far below the measured  $K_d$  for the dimer. pol  $\gamma$ B  $\Delta$ I4 would therefore be expected to be completely monomeric in these reactions, yet it functions as effectively as the

dimeric wild-type pol  $\gamma$ B and distinctly more effective than pol  $\gamma$ B  $\Delta$ I4-D129K, which is clearly a monomer. The apparent discrepancy in the properties of pol  $\gamma$ B  $\Delta$ I4 suggests that the oligomeric state of the protein may be affected by its association with pol  $\gamma$ A, either in the form of holoenzyme or in a holoenzyme-DNA complex.

We used analytical gel-filtration chromatography to reveal the oligomeric state of pol  $\gamma$ B variants. Experiments were carried out using 2  $\mu\text{M}$  pol  $\gamma$ B wild-type,  $\Delta$ I4,  $\Delta$ I4-D129K, or  $\Delta$ I4-D129K/R107E, either in the absence or presence of pol  $\gamma$ A (1  $\mu\text{M}$ ). These concentrations were expected to allow detection of changes in dimer-monomer equilibrium of  $\Delta$ I4, because they are near its  $K_d$  of 7–17  $\mu\text{M}$  (this work and Ref. 15) but far from the  $K_d$  for  $\Delta$ I4-D129K and wild-type pol  $\gamma$ B (this work), so that the  $\Delta$ I4-D129K protein is essentially entirely monomeric and the wild-type is dimeric.

Wild-type pol  $\gamma$ B (a predicted 52.5-kDa monomer) alone elutes as a molecule of  $\sim$ 100 kDa and as a singular  $\sim$ 220-kDa species when mixed with pol  $\gamma$ A (135 kDa) (Fig. 5A), consistent with complete formation of the trimeric  $\text{AB}_2$  holoenzyme. In contrast, pol  $\gamma$ B  $\Delta$ I4-D129K (50 kDa) elutes in the position expected for a 50-kDa monomer. When pol  $\gamma$ B  $\Delta$ I4-D129K is mixed with pol  $\gamma$ A and chromatographed, two individual peaks, whose apparent molecular weights correspond to each protein alone, were observed. There was no evidence for the formation of any complex, indicating that the monomeric pol  $\gamma$ B  $\Delta$ I4-D129K does not interact with pol  $\gamma$ A at this concentration. These conclusions were confirmed by analysis of the column eluate by SDS-PAGE (Fig. 5C). No pol  $\gamma$ B  $\Delta$ I4-D129K could be detected in column fractions containing pol  $\gamma$ A. Only when the concentrations of pol  $\gamma$ A and pol  $\gamma$ B  $\Delta$ I4-D129K were both raised to 4–5  $\mu\text{M}$  could any subunit interaction be detected. At this concentration,  $\Delta$ I4-D129K is still monomeric and binds to pol  $\gamma$ A to form an AB heterodimer (data not shown).

At a concentration of 2  $\mu\text{M}$ , pol  $\gamma$ B  $\Delta$ I4 is a mixture of monomer and dimer ( $\sim$ 50 and  $\sim$ 100 kDa) species (Fig. 2C). The concentration of pol  $\gamma$ B  $\Delta$ I4 dimer can be estimated from the  $K_d$  to be 0.2–0.3  $\mu\text{M}$ . In the presence of pol  $\gamma$ A, a protein species appears with an apparent molecular mass of  $\sim$ 200 kDa; this is larger than either pol  $\gamma$ A or the pol  $\gamma$ B dimer. Because  $\Delta$ I4 is a mixture of monomers and dimers, this apparent complex could be an AB heterodimer or an  $\text{AB}_2$  heterotrimer. As shown above, the monomeric  $\Delta$ I4-D129K does not bind to pol  $\gamma$ A under these conditions, and so an AB heterodimer would not be expected. The new peak, therefore, most likely contains a mixture of  $\text{AB}_2$  heterotrimeric holoenzyme and free pol  $\gamma$ A, the latter because of the substoichiometric amounts of  $\Delta$ I4 dimer. This conclusion is supported both by the facts that the new

## Processivity Enhancement by Dimerization of Accessory Subunit

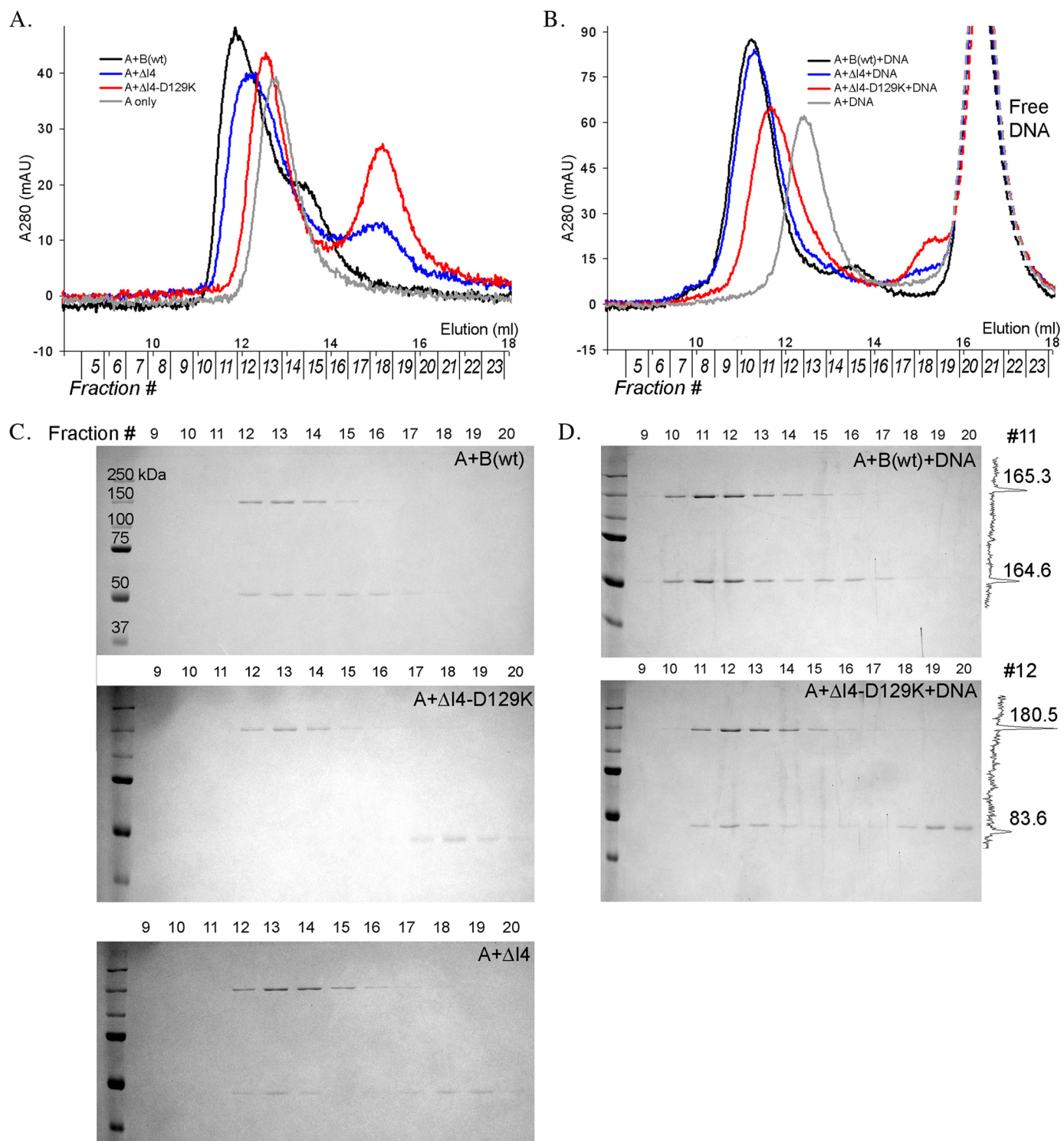


**FIGURE 5. Effects of pol  $\gamma\text{A}$  and DNA on pol  $\gamma\text{B}$  dimerization.** A, superimposed analytical gel-filtration elution profiles of 1  $\mu\text{M}$  pol  $\gamma\text{A}$  in the presence of 2  $\mu\text{M}$  wt pol  $\gamma\text{B}$  (black),  $\Delta\text{I4}$  (blue), or  $\Delta\text{I4-D129K}$  (red). The protein contents of peak fractions were visualized on SDS-PAGE gels for wt pol  $\gamma\text{B}$ ,  $\Delta\text{I4}$ , and  $\Delta\text{I4-D129K}$  (C). B, the same elution profiles as in A except that 3  $\mu\text{M}$  25/30-mer duplex DNA was included. The contents of peak fractions were analyzed on SDS gels for pol  $\gamma\text{A}$ +DNA with pol  $\gamma\text{B}$  wild-type or  $\Delta\text{I4-D129K}$  (D). Densitometry profiles of the gels are shown on the right (fraction 11 for top panel and fraction 12 for bottom panel, respectively).

peak contains both pol  $\gamma\text{A}$  and pol  $\gamma\text{B}$  and by the presence of substantial amounts of uncomplexed pol  $\gamma\text{B}$   $\Delta\text{I4}$  (Fig. 5, A and C).

These observations suggest that pol  $\gamma\text{A}$  has higher affinity for the pol  $\gamma\text{B}$  dimer than the monomer. pol  $\gamma\text{A}$  would thus pref-

erentially associate with a dimeric protein in the monomer-dimer mixture, and in doing so would bias the monomer-dimer equilibrium toward dimer formation. However, these gel-filtration experiments do not explain how pol  $\gamma\text{B}$   $\Delta\text{I4-D129K}$  can increase the polymerization amplitude of pol  $\gamma\text{A}$  in pre-steady-

state kinetic analysis. Because pol  $\gamma$ A is unable to interact with monomeric  $\Delta$ I4-D129K at 2  $\mu$ M concentration and yet stimulates pol  $\gamma$ A activity at a lower concentration, we considered the possibility that formation of a pol  $\gamma$ A-pol  $\gamma$ B holoenzyme may be affected by a primer-template DNA.

**DNA-dependent Subunit Interaction**—To examine the effect of primer-template DNA on the interaction between pol  $\gamma$ A and pol  $\gamma$ B, we repeated the analytical gel-filtration analyses in the presence of 3  $\mu$ M primer-template DNA. In contrast to the DNA-free experiments, the presence of primer-template DNA promotes complete formation of holoenzyme for both pol  $\gamma$ B  $\Delta$ I4 (Fig. 5B) and  $\Delta$ I4-D129K/R107E (not shown). The estimated molecular mass of the complex is 282 kDa, similar to that of the wild-type complex (290 kDa), indicating in both cases the formation of trimeric AB<sub>2</sub>-holoenzyme (calculated molecular masses of 235 and 240 kDa, respectively) complexed to the 16-kDa primer-template DNA.

The most dramatic changes occurred to the holoenzyme containing monomeric pol  $\gamma$ B. As described above, the monomeric pol  $\gamma$ B  $\Delta$ I4-D129K is unable to bind to pol  $\gamma$ A at 2  $\mu$ M concentration. However, a singular peak of  $\sim$ 239-kDa molecular mass was observed in the presence of DNA, and the  $A_{260}$ : $A_{280}$  ratio indicated that the peak contained DNA. Assaying column fractions by SDS-PAGE shows the presence of both pol  $\gamma$ A and pol  $\gamma$ B (Fig. 5D). The relative amounts of pol  $\gamma$ B in holoenzyme were estimated by densitometry scans of the bands corresponding to pol  $\gamma$ A and pol  $\gamma$ B on the SDS gels. The ratio of pol  $\gamma$ B:pol  $\gamma$ A for  $\Delta$ I4-D129K is about one-half that of the wild-type pol  $\gamma$ B-containing holoenzyme, providing strong evidence that  $\Delta$ I4-D129K forms an AB heterodimer. (Note that apparent molecular weights of the holoenzyme-DNA complexes are systematically overestimated, presumably due to the elongated DNA.) Increased holoenzyme formation in the presence of a primer-template fully explains the ability of the monomeric pol  $\gamma$ B  $\Delta$ I4-D129K to stimulate pol  $\gamma$ A in the pre-steady-state polymerization reaction.

## DISCUSSION

Mitochondrial DNA polymerase accessory subunits pol  $\gamma$ B are structurally and functionally different from other accessory proteins. This divergence of mitochondrial DNA replicase from prokaryotic and eukaryotic enzymes inspires many interests in evolution and structural-functional relationship of mitochondrial replication system. In contrast to the monomeric protein in lower eukaryotes, mammalian pol  $\gamma$ Bs dimerize to become a larger protein, thereby raising the question whether the extra pol  $\gamma$ B monomer yields any additional functions relating to DNA synthesis processivity.

**Contribution Factors to Processivity**—Processivity is defined as the length of DNA synthesized per enzyme binding event. It is a distance that a polymerase travels before dissociating from the template, and therefore can be expressed by two parameters,  $d = vt$ , functionally the same as  $k_{\text{pol}}/k_{\text{off}}$ , where  $v$  (or  $k_{\text{pol}}$ ) is the rate of single nucleotide incorporation reaction,  $t$  (or  $1/k_{\text{off}}$ ) is the duration of the enzyme-DNA interaction per binding event.

An accessory factor can increase processivity of a holoenzyme by either accelerating the rate of polymerization or pro-

longing the enzyme-DNA interaction. Several accessory proteins, such as the ring-shaped accessory proteins for DNA pol II and III superfamily members, and thioredoxin for T3 and T7 DNA polymerase, increase protein-DNA affinity. These processivity factors prolong the duration of holoenzyme binding to DNA but have no effect on catalysis rate (e.g. see Ref. 27). In contrast, human pol  $\gamma$ B both strengthens the binding of holoenzyme to DNA and simultaneously accelerates the rate of polymerization.

Interestingly, the catalytic subunit pol  $\gamma$ A is more processive than other polymerases, evidenced by its ability to synthesize DNA up to  $\sim$ 100 nt (28), in comparison to the 1–15 nt of other enzymes (29, 30). From a crystal structure, this high level of intrinsic processivity was attributed to a subdomain (IP) of the spacer domain that is not found in other DNA polymerases (10). However, the rate of synthesis by pol  $\gamma$ A is low, and forming a holoenzyme with pol  $\gamma$ B provides a significant rate enhancement.

Some estimates of DNA polymerase processivity have been obtained by direct visualization of product length following synthesis on a long single-stranded template in steady-state reactions where multiple cycles of nucleotide incorporation occur. Other estimates have used the ratio of the polymerization rate  $k_{\text{pol}}$  to the off-rate  $k_{\text{off}}$ , which can be obtained from pre-steady-state kinetics experiments. This method breaks processivity into two simple parameters, enabling a more detailed mechanistic dissection of processivity.

**Distinct Roles of Each pol  $\gamma$ B Monomer in Processivity**—It is conceivable that a single mode of processivity enhancement, i.e. strengthening the affinity of polymerase for DNA, can increase processivity usefully only to a certain level. For example, T7 DNA polymerase and *E. coli* pol III holoenzyme exhibit a comparable processivity, despite the great difference in the nature of their accessory subunits (16). In addition, DNA polymerases must retain some ability to dissociate from a template, and thus, if additional stimulation of processivity is needed, another mechanism may be necessary.

We have shown here that, although the proximal monomer of the human pol  $\gamma$ B dimer is solely responsible for increasing the affinity of the holoenzyme to DNA, the distal monomer is essential for the polymerization rate enhancement. These results suggest that the monomeric pol  $\gamma$ B in *Drosophila* and perhaps other lower multicellular eukaryotic organisms should have only the former activity, whereas the additional pol  $\gamma$ B monomer of mammals confers a new mode of processivity enhancement.

One reason for lack of rate enhancement by a monomeric pol  $\gamma$ B could be that an AB holoenzyme has lower affinity for dNTP. At low dNTP concentrations, the rate of synthesis by a heterodimeric AB-holoenzyme would then be slower than a heterotrimeric AB<sub>2</sub>. However, the pre-steady-state data we report were performed at a dNTP concentration (50  $\mu$ M) high enough to compensate for any theoretical increased  $K_d$  of the AB-holoenzyme. The  $K_d$  values for wild-type pol  $\gamma$ A and pol  $\gamma$  AB<sub>2</sub> holoenzyme for dNTP are 4.7  $\mu$ M and 0.9  $\mu$ M, respectively (8, 28), and it is difficult to imagine how the  $K_d$  for an AB-holoenzyme could be outside that range. The reduced rate of syn-



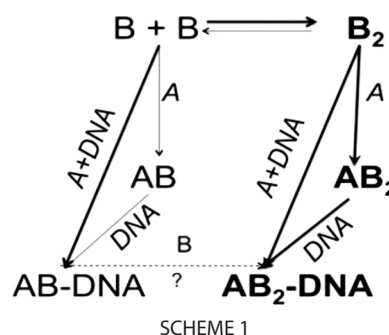
## Processivity Enhancement by Dimerization of Accessory Subunit

thesis by the AB-holoenzyme is therefore most likely due to other reasons.

Enhancement in rate of DNA synthesis occurs only when pol  $\gamma$ B is a dimer. The pol  $\gamma$ B distal monomer contacts the catalytic subunit at the exonuclease (*exo*) domain, in the vicinity of the DNA-binding channel but some distance away from the polymerization (*pol*) active site. It is therefore improbable that the distal monomer directly affects the *pol* active site conformation. Instead, its enhancement of polymerization rate is achieved either through other protein elements of pol  $\gamma$ A or by optimizing alignment of the template DNA. A modeled human pol  $\gamma$ -DNA complex suggests that binding of dimeric pol  $\gamma$ B preferentially positions the primer terminus in the *pol* active site, thereby facilitating an in-line nucleophilic attack of the primer 3'-OH on the incoming dNTP. If this model is correct, a dimeric pol  $\gamma$ B would provide a more rigid scaffold for the primer-template than could be provided by a monomer. The latter would be less effective in restricting movement of the DNA. This idea also rationalizes why the small accessory subunit thioredoxin and the toroidal sliding clamps that form flexible interactions with the catalytic subunit lack the ability to accelerate the rate of synthesis.

**pol  $\gamma$ A Promotes pol  $\gamma$ B Dimerization**—Mammalian pol  $\gamma$ B has an unusually large dimer interface of  $\sim 4000 \text{ \AA}^2$ , more than two times the size of an average protein-protein interface ( $1600 \pm 400 \text{ \AA}^2$ ) (17). We identified two regions that are critical for human pol  $\gamma$ B dimerization. Deletion of I4 in one region removes nearly half the surface contact area. However, the remaining contact area of pol  $\gamma$ B  $\Delta$ I4 is sufficiently large to support dimer formation at moderate concentrations. The estimated binding energy remaining for dimerization of  $\Delta$ I4, using a converting factor of  $25 \text{ cal/\AA}^2$ , is  $\sim 50 \text{ kcal/mol}$ . A substitution in the second region breaks two salt bridges, removing at least 8 kcal/mol binding energy. This value is probably an underestimation for the pol  $\gamma$ B D129K substitution, because the change introduces a repulsive interaction in replacement of the attractive interaction at the dimer interface. Nevertheless, D129K is not sufficient by itself to force pol  $\gamma$ B into a monomer, and both it and  $\Delta$ I4 are necessary in combination. In *Drosophila* pol  $\gamma$ B, the corresponding I4 region is partly missing, as are the residues that can make a salt bridge. We conclude that the lack of these dimerization regions result in *Drosophila* pol  $\gamma$ B being a monomer. By the same token, pol  $\gamma$ B from either mosquito or *Caenorhabditis elegans* is also predicted to be a monomer. These monomeric accessory proteins are further predicted to be able to enhance the polymerase-DNA interaction but to lack the ability to accelerate the rate of polymerization.

Dimerization of pol  $\gamma$ B is also affected by the presence of pol  $\gamma$ A. Perhaps due to the additional interactions with the distal pol  $\gamma$ B monomer, pol  $\gamma$ A preferentially binds to the dimer to form the more stable trimeric  $AB_2$ , and in doing so, shifts the pol  $\gamma$ B dimer-monomer equilibrium toward dimer formation. pol  $\gamma$ A may also directly strengthen the pol  $\gamma$ B dimer. The proximal pol  $\gamma$ B monomer becomes sandwiched between the distal monomer and pol  $\gamma$ A in the holoenzyme (Fig. 1A); by interacting with the distal pol  $\gamma$ B monomer, pol  $\gamma$ A also reinforces its interaction with the proximal monomer. Some clinical symptoms associated with the pol  $\gamma$ A R232 mutations (12, 13) may be



a consequence of this lack of reinforcement. Consequently, the patients may have less efficient mitochondrial DNA synthesis.

Regardless of the oligomeric state of pol  $\gamma$ B, the presence of a primer-template DNA further stabilizes the interactions between subunits in the holoenzyme. The effect is unlikely to be caused by pol  $\gamma$ B and pol  $\gamma$ A interacting with DNA independently, because pol  $\gamma$ B does not bind to DNA of this length (24). Rather, the interaction is most likely mediated by pol  $\gamma$ A, whose biphasic AID subdomain simultaneously binds both to the upstream DNA via a positively charged surface and to the pol  $\gamma$ B proximal monomer via a hydrophobic surface (10). The observation, that both monomeric and dimeric pol  $\gamma$ Bs show DNA-dependent holoenzyme stabilization, is consistent with the proximal monomer being solely responsible for DNA-dependent subunit interaction. Combining results from our biophysical and biochemical assays,  $\Delta$ I4 has a  $K_d$  value of  $16.6 \mu\text{M}$  but shows comparable activity to the dimeric wild-type activity at 70 nM. At this concentration the amount of dimer should be  $\sim 1 \text{ nM}$ , and we can then estimate that dimerization of pol  $\gamma$ B  $\Delta$ I4 is increased by at least 70-fold by pol  $\gamma$ A and a primer-template DNA.

The various interactions between pol  $\gamma$ A, pol  $\gamma$ B, and DNA can be summarized in Scheme 1. The catalytic subunit pol  $\gamma$ A alters the monomer-dimer equilibrium of pol  $\gamma$ B in favor of dimer formation by selectively interacting, and thus sequestering, dimeric pol  $\gamma$ B, driving more monomer into the dimer state (indicated by the *thicker arrows*). Primer-template DNA also enhances the interaction between pol  $\gamma$ A and pol  $\gamma$ B, which may then allow formation of a ternary complex to be independent of the oligomeric state of pol  $\gamma$ B. A consequence of this may be that certain mutations that destabilize the pol  $\gamma$ B dimer may have less severe clinical consequences than those that destabilize the pol  $\gamma$ A-pol  $\gamma$ B interface. The AB heterodimer preserves some capacity for processive DNA synthesis, albeit without the rate enhancement, whereas the lack of any interaction between the A and B subunits precludes all processivity enhancement. An interesting question is whether AB-DNA can be converted to the  $AB_2$ -DNA species by binding an additional monomeric pol  $\gamma$ B. With pol  $\gamma$ B  $\Delta$ I4-D129K (and perhaps *Drosophila* pol  $\gamma$ B), we imagine that it could, but at much higher concentrations than we have examined. However, the reverse reaction is more difficult to predict, because the affinities of pol  $\gamma$ B for itself (*i.e.* forming a homodimer) and for pol  $\gamma$ A (forming a heterodimer) are comparable (Refs. 15, 28, and this work). It may then be possible for  $AB_2$ -DNA to dissociate to  $(AB\text{-DNA}) + B$ ,  $(A\text{-DNA}) + B_2$ , or simply to  $A + B_2 + \text{DNA}$ .

We present here a rare example of two identical proteins that perform different functions. The species-dependent oligomeric states are thought-provoking on the evolutionary pathways leading to pol  $\gamma$ B. pol  $\gamma$ B shows obvious similarity to Class II aminoacyl-tRNA synthetases. Although modern Class II aaRSs are dimeric, the primordial enzymes are thought to be monomeric, which matches their much simpler primordial stem-loop-structured tRNA. If pol  $\gamma$ Bs indeed evolved from Class II aaRSs, their ancestors may be the primordial monomeric aaRS, as reflected by the monomeric pol  $\gamma$ B of lower eukaryotes. Subsequently, both aaRSs and the mammalian pol  $\gamma$ B independently became dimers to perform more sophisticated functions. Alternatively, pol  $\gamma$ B might have evolved after aaRSs had become dimers; in this scenario lower eukaryote pol  $\gamma$ Bs subsequently lost a monomer, whereas their mammalian counterparts remained unchanged. Dimerization of aaRSs not only accommodates the larger modern tRNA, but also potentially allows more regulation of activity. Dimerization of pol  $\gamma$ B, as we have shown in this work, may also enable an additional mechanism of processivity enhancement to the mitochondrial DNA pol  $\gamma$ A.

*Acknowledgment*—We thank Taewung Lee for constructing the pol  $\gamma$ B D129K mutant.

## REFERENCES

- Kong, X. P., Onrust, R., O'Donnell, M., and Kuriyan, J. (1992) *Cell* **69**, 425–437
- Appleton, B. A., Loregian, A., Filman, D. J., Coen, D. M., and Hogle, J. M. (2004) *Mol. Cell* **15**, 233–244
- Zuccola, H. J., Filman, D. J., Coen, D. M., and Hogle, J. M. (2000) *Mol. Cell* **5**, 267–278
- Krishna, T. S., Kong, X. P., Gary, S., Burgers, P. M., and Kuriyan, J. (1994) *Cell* **79**, 1233–1243
- Doublé, S., Tabor, S., Long, A. M., Richardson, C. C., and Ellenberger, T. (1998) *Nature* **391**, 251–258
- Hamdan, S. M., Marintcheva, B., Cook, T., Lee, S. J., Tabor, S., and Richardson, C. C. (2005) *Proc. Natl. Acad. Sci. U.S.A.* **102**, 5096–5101
- Fan, L., Sanschagrín, P. C., Kaguni, L. S., and Kuhn, L. A. (1999) *Proc. Natl. Acad. Sci. U.S.A.* **96**, 9527–9532
- Johnson, A. A., and Johnson, K. A. (2001) *J. Biol. Chem.* **276**, 38097–38107
- Farge, G., Pham, X. H., Holmlund, T., Khorostov, I., and Falkenberg, M. (2007) *Nucleic Acids Res.* **35**, 902–911
- Lee, Y. S., Kennedy, W. D., and Yin, Y. W. (2009) *Cell* **139**, 312–324
- Wernette, C. M., and Kaguni, L. S. (1986) *J. Biol. Chem.* **261**, 14764–14770
- Ferrari, G., Lamantea, E., Donati, A., Filosto, M., Briem, E., Carrara, F., Parini, R., Simonati, A., Santer, R., and Zeviani, M. (2005) *Brain* **128**, 723–731
- Kollberg, G., Moslemi, A. R., Darin, N., Nennesmo, I., Bjarnadottir, I., Uvebrant, P., Holme, E., Melberg, A., Tulinius, M., and Oldfors, A. (2006) *J. Neuropathol. Exp. Neurol.* **65**, 758–768
- Carrodeguas, J. A., Theis, K., Bogenhagen, D. F., and Kisker, C. (2001) *Mol. Cell* **7**, 43–54
- Yakubovskaya, E., Chen, Z., Carrodeguas, J. A., Kisker, C., and Bogenhagen, D. F. (2006) *J. Biol. Chem.* **281**, 374–382
- Lee, J. B., Hite, R. K., Hamdan, S. M., Xie, X. S., Richardson, C. C., and van Oijen, A. M. (2006) *Nature* **439**, 621–624
- Lo Conte, L., Chothia, C., and Janin, J. (1999) *J. Mol. Biol.* **285**, 2177–2198
- Durchschlag, H. (1986) in *Specific Volumes of Biological Macromolecules and Some Other Molecules of Biological Interest* (Hinz, H.-J., ed) pp. 45–128, Springer-Verlag, New York
- Brookes, E., Cao, W., and Demeler, B. (2009) *Eur. Biophys. J.*, Epub ahead of print
- Brookes, E., Cao, W., and Demeler, B. (2007) *GECCO Proceedings*, 978-1-59593-697-4/07/0007, ACM, New York
- Demeler, B., and Brookes, E. (2008) *Colloid Polym. Sci.* **286**, 129–137
- Demeler, B., and van Holde, K. E. (2004) *Anal. Biochem.* **335**, 279–288
- Johnson, M. L., Correia, J. J., Yphantis, D. A., and Halvorson, H. R. (1981) *Biophys. J.* **36**, 575–588
- Carrodeguas, J. A., Pinz, K. G., and Bogenhagen, D. F. (2002) *J. Biol. Chem.* **277**, 50008–50014
- Gill, S. C., and von Hippel, P. H. (1989) *Analyt. Biochem.* **182**, 319–326
- Yan, L., Ge, H., Li, H., Lieber, S. C., Natividad, F., Resuello, R. R., Kim, S. J., Akeju, S., Sun, A., Loo, K., Peppas, A. P., Rossi, F., Lewandowski, E. D., Thomas, A. P., Vatner, S. F., and Vatner, D. E. (2004) *J. Mol. Cell Cardiol.* **37**, 921–929
- Huber, H. E., Tabor, S., and Richardson, C. C. (1987) *J. Biol. Chem.* **262**, 16224–16232
- Johnson, A. A., Tsai, Y., Graves, S. W., and Johnson, K. A. (2000) *Biochemistry* **39**, 1702–1708
- Hori, K., Mark, D. F., and Richardson, C. C. (1979) *J. Biol. Chem.* **254**, 11591–11597
- McHenry, C., and Kornberg, A. (1977) *J. Biol. Chem.* **252**, 6478–6484